

Supplement of Atmos. Chem. Phys., 16, 13309–13319, 2016  
<http://www.atmos-chem-phys.net/16/13309/2016/>  
doi:10.5194/acp-16-13309-2016-supplement  
© Author(s) 2016. CC Attribution 3.0 License.



Atmospheric  
Chemistry  
and Physics  
Open Access  
EGU

*Supplement of*

## **The climatology of planetary boundary layer height in China derived from radiosonde and reanalysis data**

**Jianping Guo et al.**

*Correspondence to:* Jianping Guo (jpguocams@gmail.com) and Zhanqing Li (zli@atmos.umd.edu)

The copyright of individual parts of the supplement might differ from the CC-BY 3.0 licence.

## Contents

**Figure S1.** Spatial distribution of near-surface 0800 BJT wind speed (a) in spring, and the wind speed difference (subtracted from that of spring) in (b) summer, (c) fall, and (d) winter. The seasonally averaged near-surface wind speed was obtained from the CMA soundings by averaging the observations below 100 m AGL.

**Figure S2.** Similar as Figure R1, but for the spatial distribution of near-surface wind speed at 2000 BJT.

**Figure S3.** Spatial distribution of near-surface inversion strength (vertical potential temperature gradient between 10 m and 100 m AGL) at 0800 BJT in (a) spring, (b) summer, (c) fall, and (d) winter.

**Figure S4.** Spatial distribution of seasonally averaged 10-m wind speed in (a) spring, (b) summer, (c) fall, and (d) winter derived from ERA-Interim reanalysis from January 2011 to July 2015.

**Figure S5.** Spatial distributions of seasonally averaged ERA-BLH (color shaded) and CMA-BLH (color dots) at (a) 0200 BJT, (b) 0800 BJT, (c) 1400 BJT, and (d) 2000 BJT in spring.

**Figure S6.** Same as Figure S3, but for spatial distributions of BLHs in fall.

**Figure S7.** Same as Figure S3, but for spatial distributions of BLHs in winter.

**Figure S8.** Monthly mean of CMA-BLH at Beijing (39.8 °N, 116.47 °E) from January 2011 to July 2015 at 0800 BJT (dot symbols) and 2000 BJT (x symbols), respectively, as superimposed by the counterparts of meteorological parameters, including (a) surface pressure (Ps), (b) 10-m wind speed (WS), (c) near-surface temperature (Ts), and (d) Lower Tropospheric Stability (LTS). The correlation coefficients at 0800 (R08) and 2000 BJT (R20) between of CMA-BLH and meteorological parameters are given in each

panel as well, and the star superscripts indicate the values that are statistically significant ( $p < 0.05$ ).

**Figure S9.** Correlations (R) between monthly mean values (from January 2011 to July 2015) of CMA-BLH and (a, b) surface pressure (Ps), (c, d) 10-m wind speed, (e, f) near-surface temperature (Ts), (g, h) Lower Tropospheric Stability (LTS), at (left) 0800 and (right) 2000 BJT. Symbols outlined in black indicate values that are statistically significant ( $p < 0.05$ ).

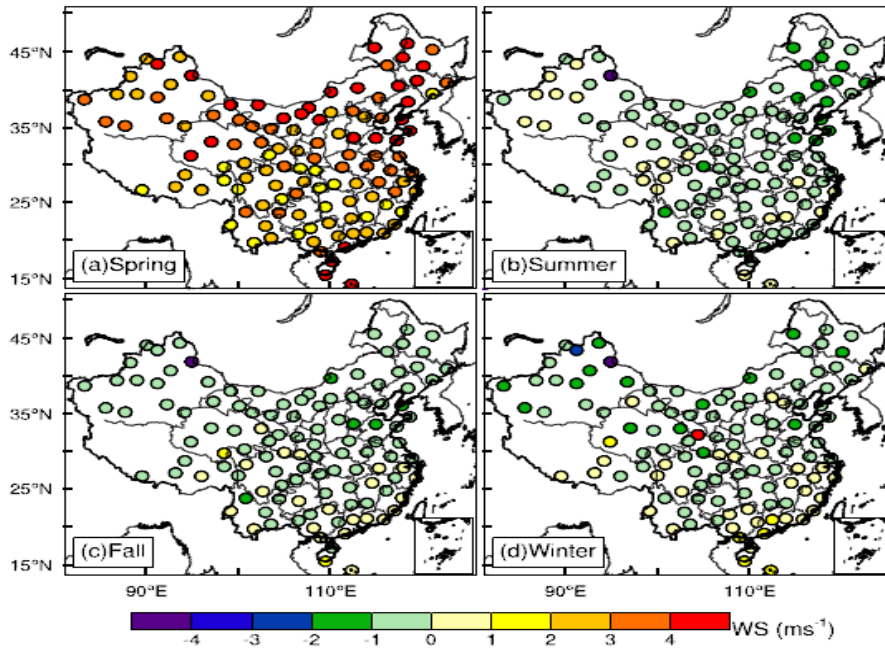


**Figure S1.** Spatial distribution of near-surface 0800 BJT wind speed (a) in spring, and the wind speed difference (subtracted from that of spring) in (b) summer, (c) fall, and (d) winter. The seasonally averaged near-surface wind speed was obtained from the CMA soundings by averaging the observations below 100 m AGL.

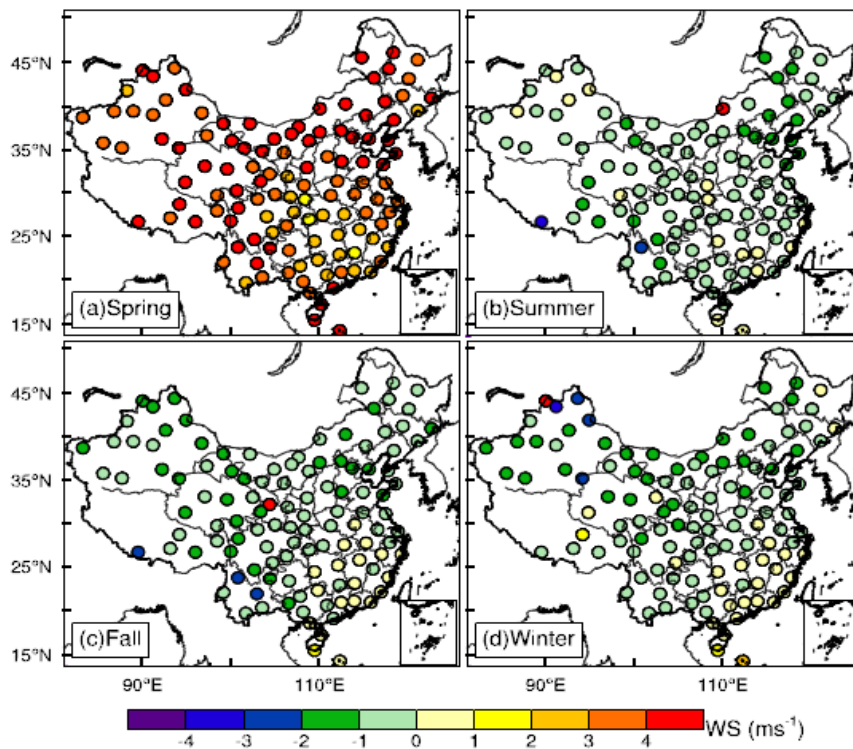


**Figure S2.** Similar as Figure R1, but for the spatial distribution of near-surface wind speed at 2000 BJT.

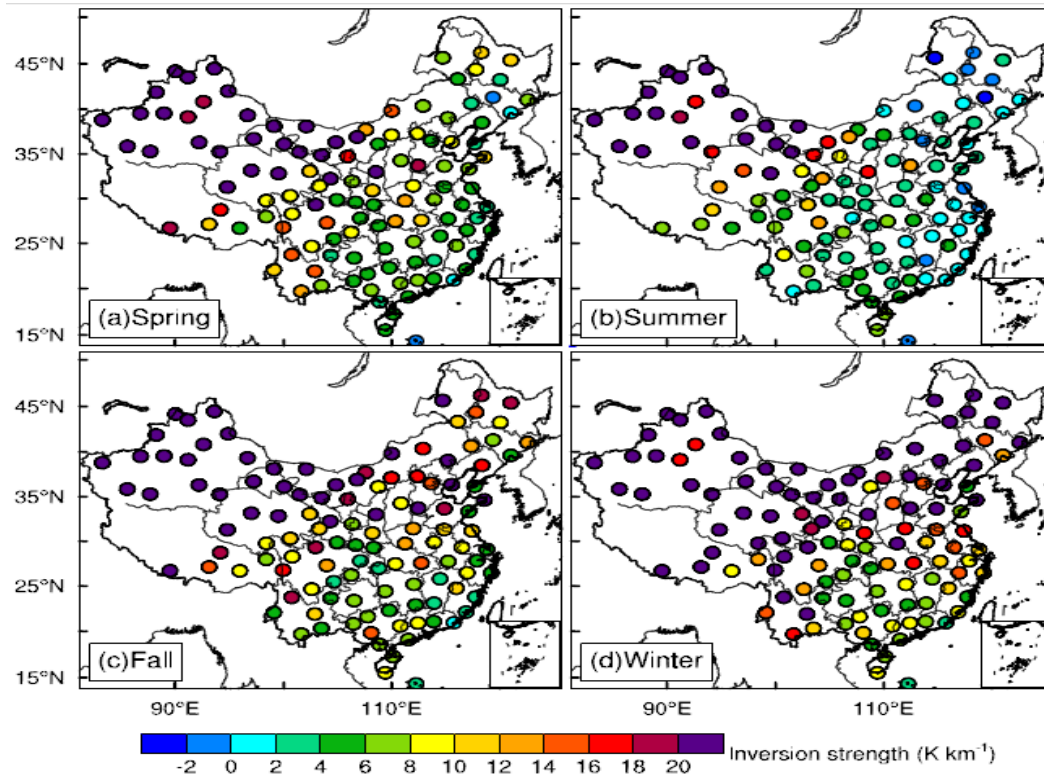


**Figure S3.** Spatial distribution of near-surface inversion strength (vertical potential temperature gradient between 10 m and 100 m AGL) at 0800 BJT in (a) spring, (b) summer, (c) fall, and (d) winter.

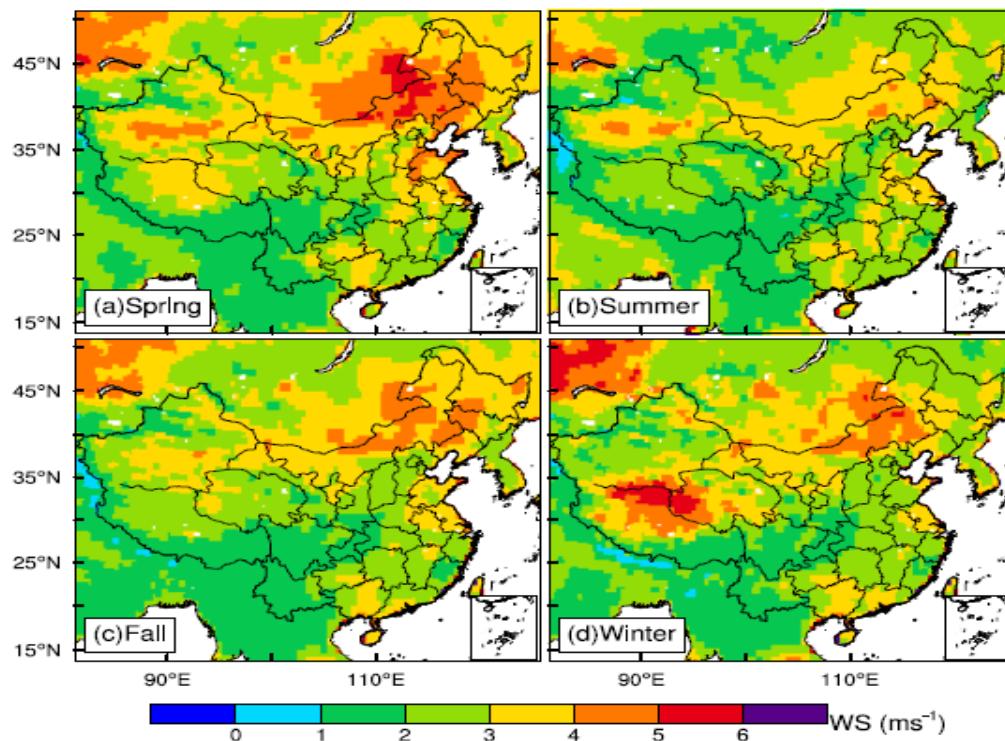


**Figure S4.** Spatial distribution of seasonally averaged 10-m wind speed in (a) spring, (b) summer, (c) fall, and (d) winter derived from ERA-Interim reanalysis from January 2011 to July 2015.

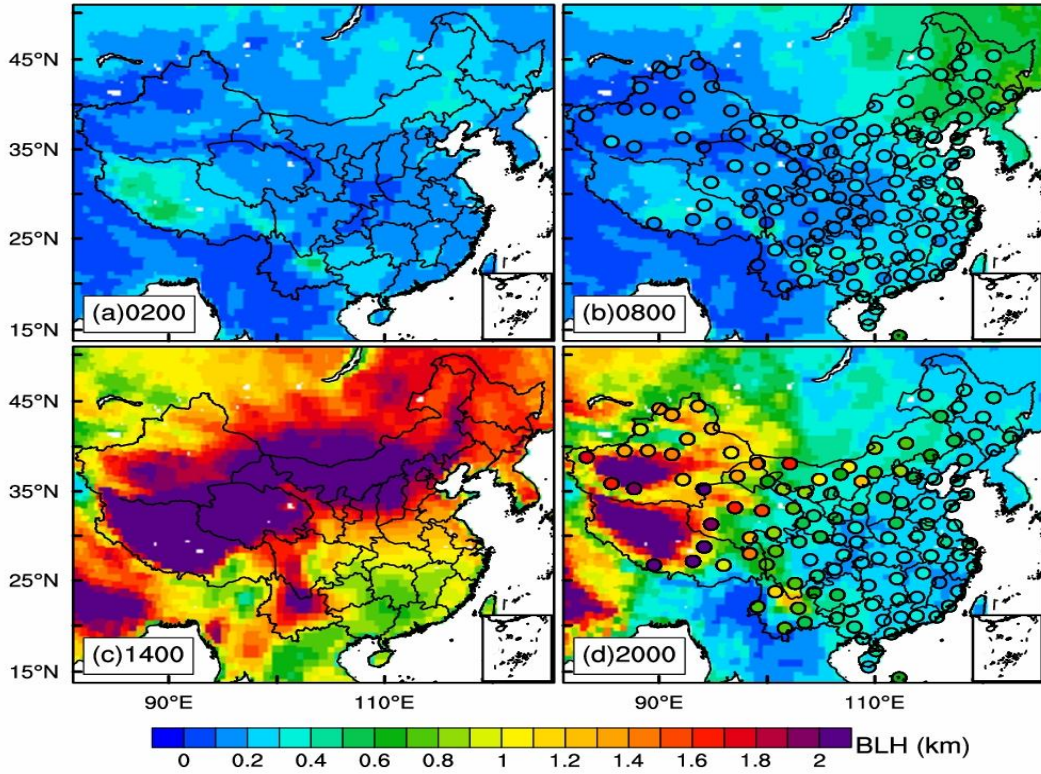


**Figure S5.** Spatial distributions of seasonally averaged ERA-BLH (color shaded) and CMA-BLH (color dots) at (a) 0200 BJT, (b) 0800 BJT, (c) 1400 BJT, and (d) 2000 BJT in spring.

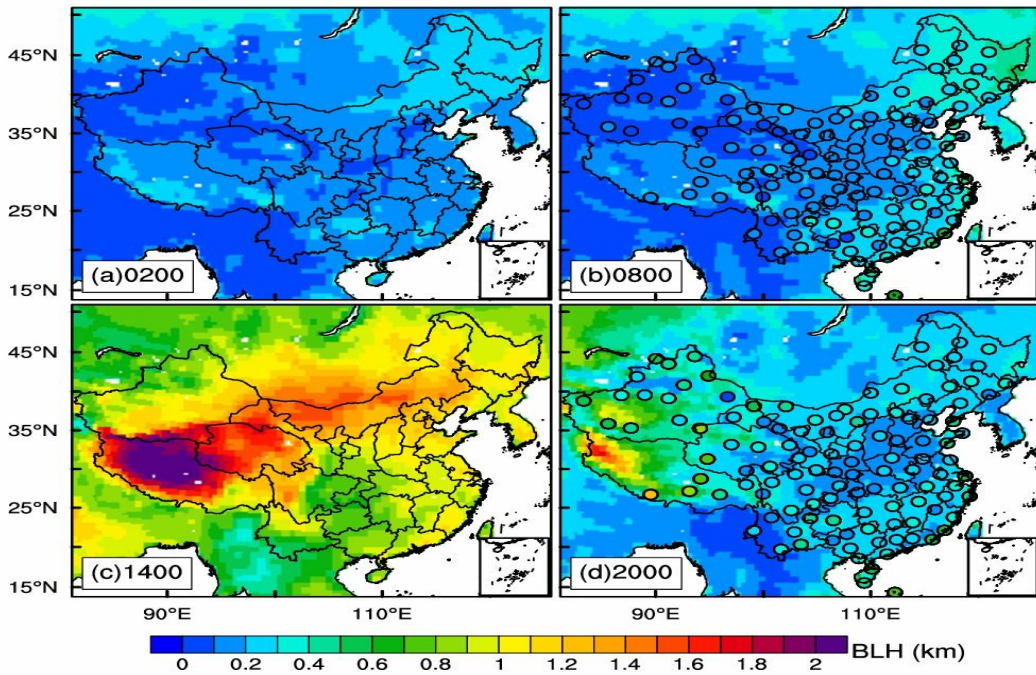


**Figure S6.** Similar as Figure S3, but for spatial distributions of BLHs in fall.

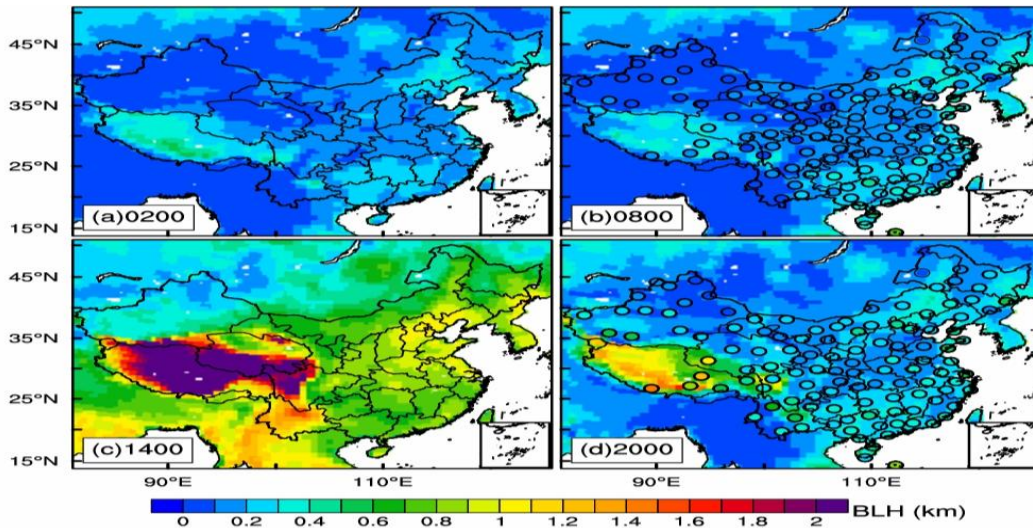


**Figure S7.** Similar as Figure S3, but for spatial distributions of BLHs in winter.

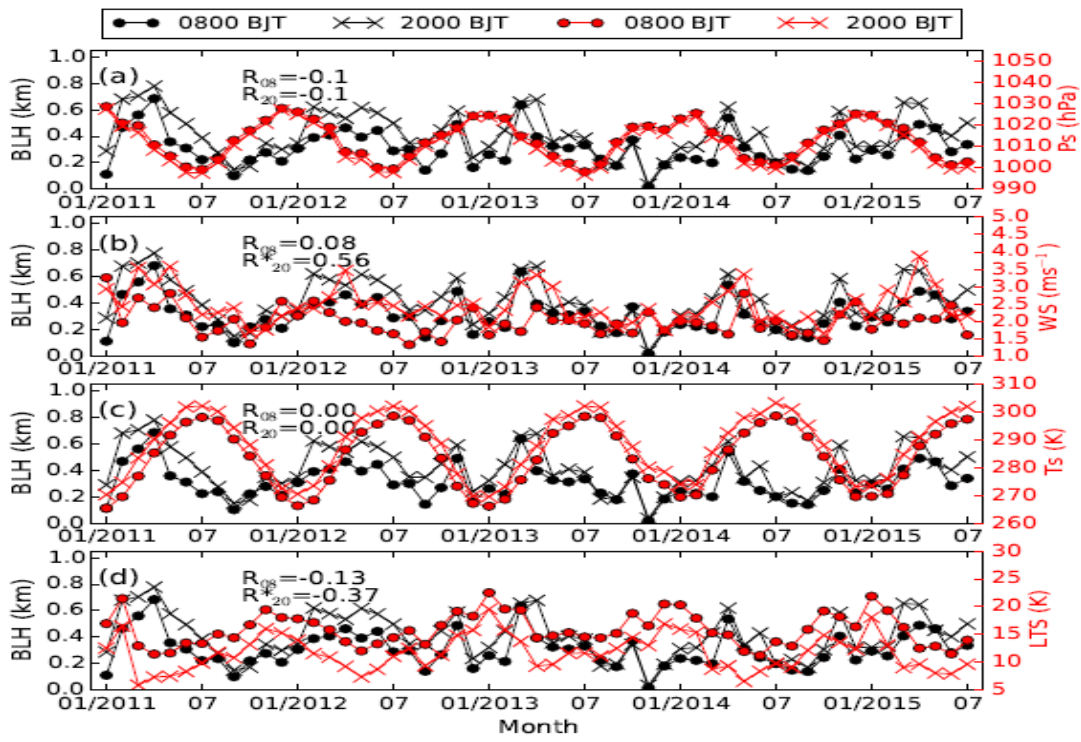


**Figure S8.** Monthly mean of CMA-BLH at Beijing ( $39.8^{\circ}\text{N}$ ,  $116.47^{\circ}\text{E}$ ) from January 2011 to July 2015 at 0800 BJT (dot symbols) and 2000 BJT (cross symbols), respectively, as superimposed by the counterparts of meteorological parameters, including (a) surface pressure ( $P_s$ ), (b) 10-m wind speed ( $WS$ ), (c) near-surface temperature ( $T_s$ ), and (d) Lower Tropospheric Stability ( $LTS$ ). The correlation coefficients at 0800 ( $R_{08}$ ) and 2000 BJT ( $R_{20}$ ) between of CMA-BLH and meteorological parameters are given in each panel as well, and the star superscripts indicate the values that are statistically significant ( $p < 0.05$ ).

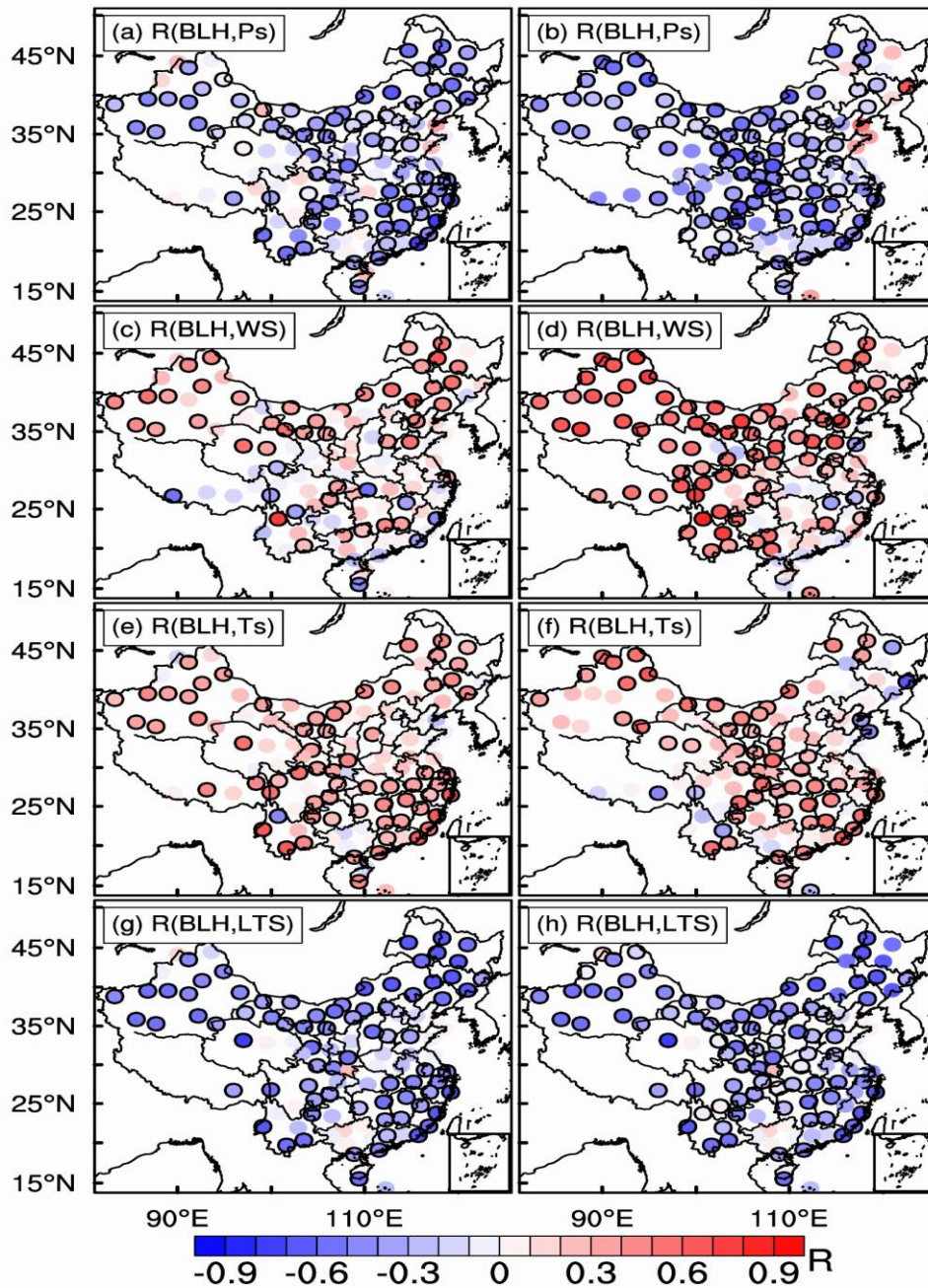


**Figure S9.** Correlations ( $R$ ) between monthly mean values (from January 2011 to July 2015) of CMA-BLH and (a, b) surface pressure ( $P_s$ ), (c, d) 10-m wind speed, (e, f) near-surface temperature ( $T_s$ ), (g, h) Lower Tropospheric Stability (LTS), at (left) 0800 and (right) 2000 BJT. Symbols outlined in black indicate values that are statistically significant ( $p < 0.05$ ).